

# Enhanced Brain Tumor Segmentation via Transfer Learning and Attention Mechanism

1<sup>st</sup> Ilyasse Aboussaleh

LISAC Laboratory, Department of  
Computer Science, Faculty of Sciences  
Dhar El Mahraz, University Sidi  
Mohamed Ben Abdellah  
LISAC Laboratory  
Fez, Morocco  
aboussalehilyasse@gmail.com

2<sup>nd</sup> Jamal Riffi

LISAC Laboratory, Department of  
Computer Science, Faculty of Sciences  
Dhar El Mahraz, University Sidi  
Mohamed Ben Abdellah  
LISAC Laboratory  
Fez, Morocco  
riffi.jamal@gmail.com

3<sup>rd</sup> Khalid El Fazazy

LISAC Laboratory, Department of  
Computer Science, Faculty of Sciences  
Dhar El Mahraz, University Sidi  
Mohamed Ben Abdellah  
LISAC Laboratory  
Fez, Morocco  
khalid.elfazazy@usmba.ac.ma

4<sup>th</sup> Mohamed Adnane Mahraz

LISAC Laboratory, Department of  
Computer Science, Faculty of Sciences  
Dhar El Mahraz, University Sidi  
Mohamed Ben Abdellah  
LISAC Laboratory  
Fez, Morocco  
adnane\_1@yahoo.fr

5<sup>th</sup> Hamid Tairi

LISAC Laboratory, Department of  
Computer Science, Faculty of Sciences  
Dhar El Mahraz, University Sidi  
Mohamed Ben Abdellah  
LISAC Laboratory  
Fez, Morocco  
hamid.tairi@usmba.ac.ma

**Abstract**— Brain tumor segmentation involves the crucial process of distinguishing diseased regions within the brain from healthy tissue in medical imaging, playing a crucial role in diagnosis and treatment planning for brain tumors. Deep learning, particularly encoder-decoder architectures, has recently demonstrated significant advancements in this field. This study explores the application of transfer learning and the attention mechanism to develop various models for brain tumor segmentation tasks. By fine-tuning three established pre-trained models (VGG19, ResNet50, and MobileNetV2) during the encoder phase, we aim to enhance the recognition of pertinent features for this specific task. Additionally, integrating the attention mechanism in the decoder phase enables selective focus on specific features within the input feature map, facilitating the preservation of fine details while disregarding irrelevant information. Extensive experiments are conducted on the publicly available BraTS2020 dataset, yielding promising results characterized by high accuracy and dice similarity coefficient scores.

**Keywords**—brain tumor, segmentation, deep learning, transfer learning, attention.

## I. INTRODUCTION

Medical imaging analysis is pivotal in diagnosing brain tumors, aiding patient care, and preserving lives. Modern imaging technologies, including positron emission tomography (PET), computed tomography (CT), and magnetic resonance imaging (MRI), contribute significantly to accurate diagnoses. MRI, in particular, offers various modalities such as T1-weighted, T2-weighted, T1 contrast-enhanced (T1c), and fluid-attenuated inversion recovery (FLAIR), each providing unique insights into brain tissue's structural and functional characteristics. These modalities typically present as 2D slices, with the compilation of these slices enabling the creation of a comprehensive 3D representation of the brain's structure. Based on these technologies, automated approaches have not only shown their performance but also a strong potential for more accurate and robust results. This potential, driven by unsupervised and supervised methods based on machine learning algorithms, is a promising development in the field. Almahfud et al. [1] combined two basic algorithms, K-Means, and Fuzzy C-Means, to enhance image visibility; after that, they mapped the resulting image, applied a median

filter, and used the opening morphological technique for more accuracy. The feature engineering phase remains the most crucial in ML, and the right choice of features makes the constructed model more robust. For that matter, Cui et al. [2] used an intensity texture for feature extraction after image registration in the first step of preprocessing. Next, they employed a multi-kernel support vector machine (SVM) as a classifier. Chen et al. [3] chose the gray statistic and gray level co-occurrence matrix for feature extraction and SVM as a classifier. They are also used for preprocessing, simple linear iterative clustering, and histogram matching. For the methods [4,5], the random forest (RF) has been chosen for the classification phase and morphological techniques with thresholding in the post-processing step to ameliorate the results of tumor segmentation. The difference between these two methods was in the features-extracting phase. Therefore, the first was based on the first higher-order and texture, while the second employed histogram enhancement and Gabor wavelet. Intensity inhomogeneity in MRI imaging complicates phase extraction of features in ML methods, and the amount of such data affects the performance and limits the results of most ML algorithms. However, deep learning has emerged as a promising solution to overcome these limitations, and it has showcased its prowess in analyzing and retrieving medical images [6,7], particularly excelling in the segmentation of medical images. This reassures us about the progress in the field. Convolutional neural networks (CNNs) and autoencoders (AEs) represent the cornerstone of research in this domain. Pereira et al. [8] introduced a CNN-based approach, emphasizing the utilization of small kernels for designing deeper architectures. This strategy mitigated overfitting due to the network's reduced weights and enhanced performance. Additionally, they investigated the effectiveness of intensity normalization as a preprocessing step, coupled with data augmentation, for robust brain tumor segmentation in MRI images. Other methodologies [9,10] incorporate full CNN architectures to segment distinct tumor regions. In one instance [9], a combination of fully convolutional neural networks (FCNNs) and conditional random forest (CRF) was proposed. At the same time, another study [10] suggested a cascade of FCNNs to segment individual tumor sub-regions, yielding three binary segmentations. Aboussaleh et al. [11] utilized features

extracted from the final convolutional layer of a CNN-based model, followed by post-processing of the segmented tumor using thresholding with the opening morphological process. On the other hand, Ronneberger et al. [12] proposed U-Net, a symmetric, fully convolutional network with two paths: encoder and decoder; the first is for capturing the context information, and the second is for ensuring precise position. U-Net and her symmetric methods have succeeded and wildly succeeded in segmentation problems, especially in medical image segmentation. This success inspires us about the potential of these techniques in our field. In this paper, three different architectures have been developed based on U-Net. We applied transfer learning in the encoder part by fine-tuning three different pre-trained models: VGG19, ResNet50 and MobileNetV2 to extract more pertinent features, and we introduced the attention mechanism in the decoder part for more attention on the tumor's area. We have carried out an ablation study and a comparative study between these methods including the basic method U-Net, and we found that the transfer learning and the attention mechanism augment the performance of the results in term of accuracy and dice similarity coefficient. Section 2 is the description of the related works, and section 3 is the presentation of the materials and method. Then, section 4 is for representing results and discussion. Finally, section 5 is considered as the conclusion of this study.

## II. RELATED WORK

The U-Net architecture continues to serve as a benchmark for 2D and 3D brain tumor segmentation, inspiring numerous variations through modifications to the encoder, skip connections, or decoder components. For instance, Liu et al. [13] introduced a cascaded U-Net method featuring residual blocks to address the vanishing gradient issue and multiple skip connections facilitating the transfer of high-resolution information across network layers. Aboelenen et al. [14] merged two U-Net tracks, employing leaky ReLU activation and batch normalization, with each track possessing a distinct layer count and kernel size. Furthermore, Aboussaleh et al. [15] developed U-Det [16] architecture by improving the skip connection path. However, they employed an inception block instead of a convolution one to get more parallelized and pertinent patterns, besides optimizing the number of parameters. Recent advancements have seen U-Net combined with transfer learning to tackle complex challenges such as computational inefficiency and large dataset requirements. Additionally, CNN architectures like VGGNet, LeNet, AlexNet, MobileNet, and ResNet have been integrated into various methods, such as the UNet-VGG16 proposed by Pravitasari et al. [17], demonstrating promising performance. However, these approaches still need to capture global semantic information essential for segmentation tasks, prompting the introduction of attention mechanisms to address this issue. Zhang et al. [18] investigated the effectiveness of the Attentional Gate module within a U-Net framework, resulting in the AGResU-Net architecture, which integrates residual modules and attention gates to emphasize salient features. Similarly, Aboussaleh et al. [19] employed attention mechanisms in the decoder phase of their method,

leveraging multiple pre-trained models and a bi-directional features pyramid network after extracting pertinent features from the encoder phase. Additionally, the authors proposed a 3D hybrid encoder-decoder model [20] based on the features extracted from both U-Net and V-Net and Transformers blocks in the decoder to extract more contextual features and achieve high segmentation results. On the other hand, Wu et al. [21] proposed an unsupervised method for brain tumor segmentation; it is named a symmetric-driven generative adversarial network (SD-GAN). The method has been used to reconstruct the non-tumor brains and segment the abnormal ones based on the error calculated from their being unsymmetrical.

## III. MATERIALS AND METHOD

### A. Dataset

The BraTS dataset [22-24] is a widely recognized benchmark in medical image analysis, especially for brain tumor segmentation tasks. It includes a collection of MRI scans of the brain featuring T1-weighted, T2-weighted, and T1-weighted with contrast-enhancement (T1c) and fluid-attenuated inversion recovery (FLAIR) sequences. A total of 285 scans are available, with 160 used for training and 125 for validation. Each MRI scan comes with detailed manual segmentation labels, delineating various brain tumor regions, such as necrosis, edema, enhancing tumor, and non-enhancing tumor.

### B. Data preprocessing

We have processed each patient's BraTS 2020 dataset by resizing it from a 3D to a 2D ( $240 \times 240 \times 155$  to  $240 \times 240$ ) image by selecting the middle slice of each modality, cropping it to remove insignificant background pixels, applying Gaussian denoising, and normalizing the image by subtracting its mean. We then divided it by its standard deviation to obtain Equation 1. We applied data augmentation to our dataset to generate more training data and prevent overfitting.

$$i_0 = \frac{i - \mu}{\sigma} \quad (1)$$

### C. Method

In our paper, the encoder part of each architecture adopts the use of fine-tuning technique, by deleting the classification layers and retrain the weights of all convolutional and pooling layers. More details of the architectures are illustrated in Fig 3.4. and 5.

- *VGG19*

In 2014, the Visual Geometry Group at the University of Oxford introduced VGG19 as a convolutional neural network architecture. It is known for its good performance in image classification tasks and its deep network structure. The network is composed of 19 layers, including 16 convolutional layers and 3 fully connected layers. It is characterized by the use of small convolutional filters (3x3) and a deep network structure, allowing the network to learn hierarchical representations of the input.

- *ResNet50*

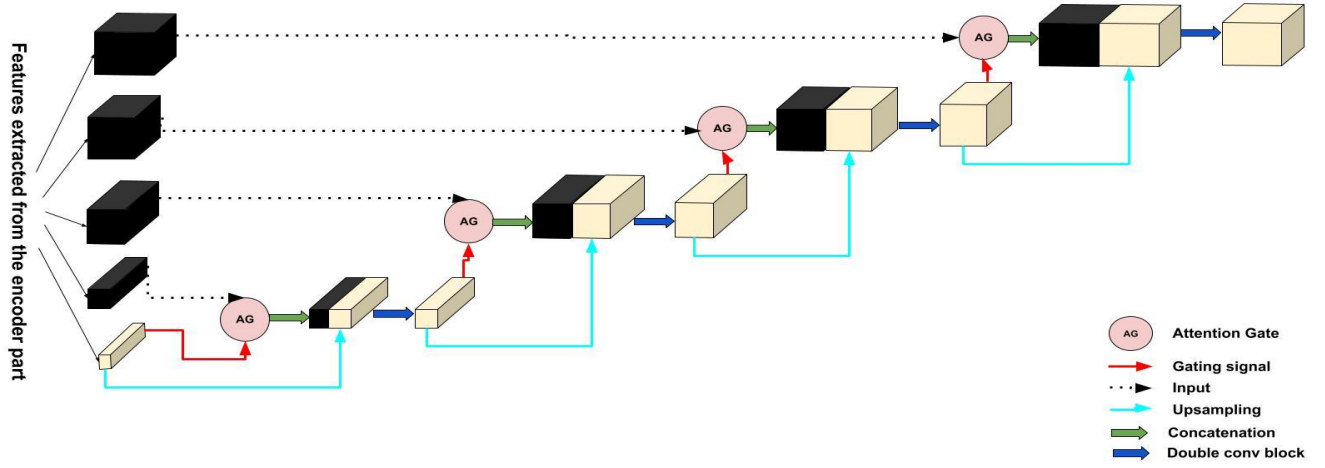


Fig. 1. Schematic of the attention decoder proposed.

ResNet50 is a deep residual neural network architecture introduced in 2015. It was designed to address the vanishing gradient problem that affects deep neural networks. The architecture consists of 50 convolutional layers and is trained on Image Net data to perform image classification. A residual block in ResNet50 consists of two convolutional layers, each followed by batch normalization and a ReLU activation. The residual connection is added between the input and output of the block, allowing the network to learn residual functions instead of direct mapping.

- *MobileNetV2*

MobileNetV2 is a deep learning architecture that is designed to run efficiently on mobile and embedded devices. It was introduced in 2018 as a successor to MobileNetV1 and is characterized by its lightweight, efficient structure and strong accuracy performance. The architecture of MobileNetV2 is based on depthwise separable convolutions, which divide the standard convolution operation into two separate stages: depthwise convolution and pointwise convolution. This allows the network to maintain a relatively small number of parameters while still achieving high accuracy.

- *Attention decoder*

The incorporation of an attention mechanism within the decoder of an image segmentation model allows the model to selectively focus on the most relevant regions of the input image. This capability is particularly valuable for handling large and intricate images, as well as enhancing performance when the objects of interest are only a small portion of the overall image. Our proposed deconvolution block starts with an attention block, proceeds with an upsampling step to increase the dimensionality, and concludes with a double convolution layer block. This block incorporates a batch normalization layer and is activated using the ReLU activation function.

Inspired by the human attention mechanism, the attention block, or attention gate (AG) feature maps, thereby highlighting task-specific meaningful information. Fig.2 provides a schematic representation of the attention-block.,

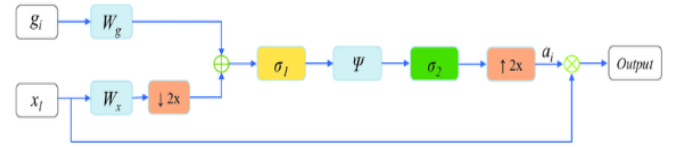


Fig. 2. Schematic of the attention gate.

Where  $x_l$  is the feature map of the  $l$  layer,  $g_l$  a gating signal vector, is used for each pixel  $i$  in order to select the focus regions on a coarser scale. The attention coefficient  $\alpha_i$  belongs to the interval  $[0; 1]$ . It highlights the essential regions of the image while excluding unnecessary pixels, retaining only the activation features relevant to the specific segmentation task. The AG output is the wise-multiplication between the attention coefficient  $\alpha_i$  and the feature map  $x_l$ .

$$x_{output} = x_l \cdot \alpha_i \quad (2)$$

$$\alpha_i = \sigma_2 \left( \psi^T \left( \sigma_1 (W_x^T x_l + W_g^T g_l + b_g) \right) \right) + b_\psi \quad (3)$$

Where  $\sigma_1$  is defined as a ReLU function  $\sigma_1(x) = \max(0, x)$  and  $\sigma_2$  is the Sigmoid function  $\sigma_2(x) = \frac{1}{1+e^{-x}}$ .  $W_x$ ,  $W_g$  and  $\psi$  are linear transformations, and  $b_g$  and  $b_\psi$  are bias terms. The AG output will be concatenated with the up-sampled bottleneck, and a double convolution is affected to the concatenation result, the same process will be applied in each depth of the encoder, to complete the decoder attention proposed. Fig.1 showed the details of our proposed attention decoder.

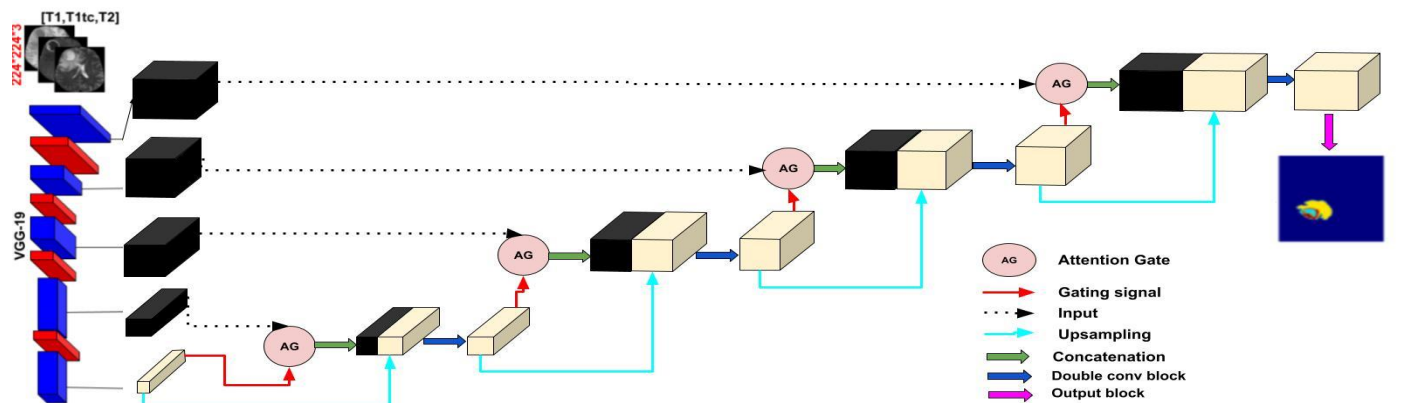


Fig. 3. Schematic of the proposed method using Vgg19 pretrained model as encoder and Attention decoder.

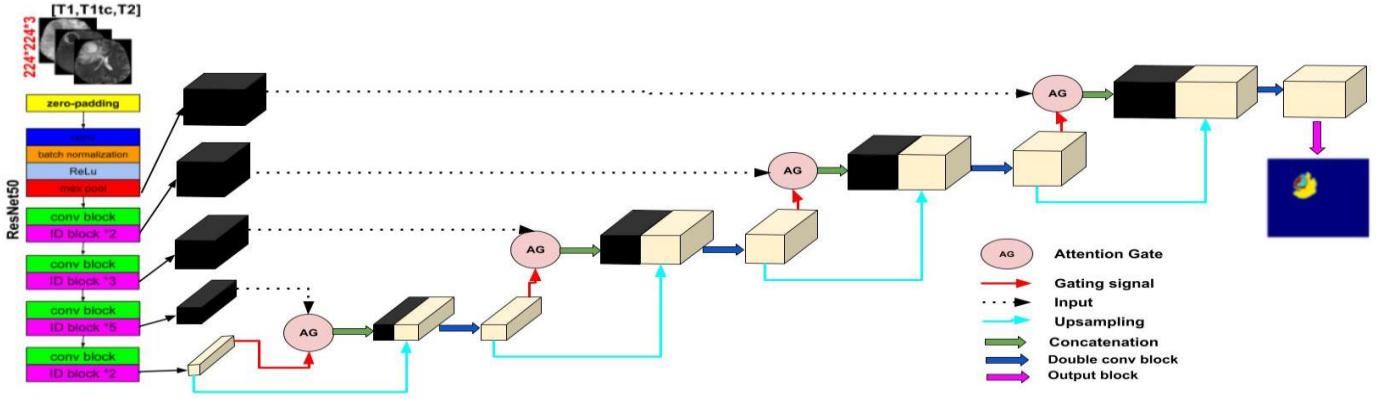


Fig. 4. Schematic of the proposed method using ResNet50 pretrained model as encoder and Attention decoder.

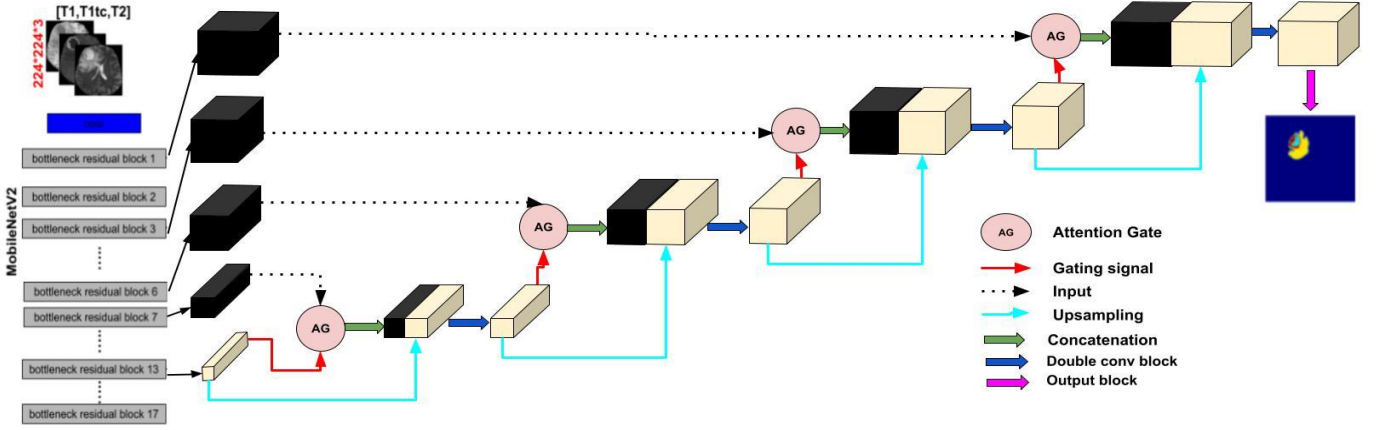


Fig. 5. Schematic of the proposed method using MobileNetV2 pretrained model as encoder and Attention decoder.

#### IV. RESULTS AND DISCUSSION

##### A. Implementation details

In this experiment, we used SIMPLSTIK, an image analysis toolkit with many components supporting everyday filtering operations, image segmentation, and registration, to read MRI images from BraTS2020 data with NIFTI format type. We have chosen three sequences among the four possible (t1, t2, T1ce, Flair) to adopt the recommended dimension of the pre-trained models that will be used, which makes the number of possible cases, keeping the importance of the order 24. To address this, Kronberg et al. [25] proposed the optimal sequence order following a comprehensive comparison of all possible scenarios, including cases with the absence of one or more sequences. According to their findings, the recommended sequence order is [t1, t1ce, t2], with the caveat that the 90th slice out of 155 is selected for each sequence. The loss function used for our model was the Dice Loss [26] by computing the following average:

$$Dice(P, G) = \frac{2 \sum_{i=1}^N p_i g_i}{\sum_{i=1}^N p_i^2 + \sum_{i=1}^N g_i^2} \quad (4)$$

where  $P$  is the predicted value and  $G$  stands for the mask which represents the ground truth.  $p_i \in P$  and  $g_i \in G$ . We used Adam optimizer to minimize this loss function, with initial learning rate of  $\alpha_0 = 10^{-4}$  and progressively decreased it according to:

$$\alpha = \alpha_0 \times \left(1 - \frac{e}{N_e}\right)^{0.9} \quad (5)$$

where  $e$  is an epoch counter and  $N_e$  is the total number of epochs, in our case, the maximum number of epochs = 350, and the batch size employed is 5.

##### B. Evaluation metrics

In evaluating the performance of our segmentation model on the BraTS dataset, we utilize accuracy and Dice Similarity Coefficient (DSC) metrics to assess the accuracy of tumor segmentation and measure the agreement between predicted and ground truth tumor regions:

- Accuracy: Formally, accuracy is defined as follow:

$$Accuracy = \frac{TruePositive + TrueNegative}{Total} \quad (6)$$

- DSC measures the overlap between the predicted (S) and ground truth segmentation masks (G), providing a measure of segmentation accuracy. It ranges from 0 (no overlap) to 1 (perfect overlap):

$$DSC = 2 \times \frac{|G \cap S|}{|G| + |S|} \quad (7)$$

##### C. Results and discussion

In this subsection, we will present all the results derived from our methods, conduct an analysis of these findings, compare them with select state-of-the-art methods, and illustrate some qualitative results. To assess our model's

performance, we partitioned the BraTS 2020 training dataset into three subsets: training, validation, and test, with an 80:10:10 ratio. TABLE I shows the metrics of the proposed methods on test sub-set after training all the models in training sub-set and validating them on the validation sub-set. The encoder of each approach employs a pretrained model with two different decoders. The first decoder contains an upsampling operation, followed by concatenation and a convolution operation. The second is the attention decoder which is explained in the section of materials and method. We also implemented the basic U-Net method and we evaluated all the performances for each case. A high accuracy was mentioned for each method that demonstrates the strength of the U-Net-like architectures in image segmentation problems. A good performance was illustrated in terms of DCS of each tumor sub-region and the whole tumor in particular.

TABLE I. METRICS OF THE PROPOSED METHODS USING CONVOLUTION DECODER AND OUR PROPOSED ATTENTION DECODER ON BRATS 2020 TEST SUB-SET

Method	WT <sup>a</sup>	DSC (%) TC <sup>b</sup>	EnT <sup>c</sup>	Accuracy (%)AVG <sup>d</sup>
U-Net	80	62	60	92
U-Net with attention decoder	82.22	68.6	65.44	97
Vgg19+ConvDecoder	80.77	74.22	60.03	98
Vgg19+AttentionDecoder	81.32	75.13	61.66	98
ResNet50+ Conv Decoder	85.34	76.55	68.22	99
ResNet50+ Attention Decoder	86.49	78.98	70.90	99
MobileNetV2+ Conv Decoder	86.51	79.48	68.12	99
MobileNetV2+ Attention Decoder	86.89	82.02	71.34	99

<sup>a</sup>. "WT" stands for "WHOLE TUMOR"

<sup>b</sup>. "TC" stands for "CORE TUMOR"

<sup>c</sup>. "EnT" stands for "ENHANCING TUMOR"

<sup>d</sup>. "AVG" stands for "average"

TABLE II showed a comparison study between our proposed methods and some methods from the state of art section and some others out of the state of art. The results obtained are very close to each other, especially the methods belonging to the U-Net-like architecture, a high DSC of whole tumor is gated by AGResU-Net, ResNet50+AttD, and MobilNetV2+AttD. The latter gets the best performance of 82.02% for the core tumor segmentation and a satisfied result of 71.34% for enhancing sub-region, the hardest type to segment.

TABLE II. PERFORMANCE COMPARISON BETWEEN OUR METHODS AND DIFFERENT SUPERVISED AND NON SUPERVISED APPROACHES ON BRATS DATASET

Method	Data	WT	DSC (%) TC	EnT
Single-Path MLDeepMedic [29]	BraTS2017	79.73	71.59	68.14
Fang et al [27]	BraTS2018	85.60	72.20	72.60
Chen et al [28]	BraTS2018	83.60	68.90	78.30
U-Net [13]	BraTS2020	80	62	60
HTTU-Net [15]	BraTS2018	86.50	74.50	80.80
AGResU-Net [22]	BraTS2019	87	77.70	70.90
Vgg19+AttD <sup>a</sup> (ours)	BraTS2020	81.32	75.13	61.66

ResNet50+AttD(ours)	BraTS2020	86.49	78.98	70.90
MobilNetV2+AttD(ours)	BraTS2020	86.89	82.02	71.34

<sup>a</sup>. "AttD" means "Attention Decoder"

Qualitative results are shown in Fig. 6, to verify and visualize our work. The three first images vertically correspond to the three modalities chosen as input from four possible as; T1, T1ce, and T2, followed by the output of each approach Vgg19+AttD, ResNet50+AttD, and MobilNetV2+AttD respectively, and the final image is the ground truth of each input image. The visualization obtained is significant with some marks to mention. On a global scale, the segmentation of the entire tumor has been executed with high accuracy, while the images devoid of tumors also exhibit commendable results. Also, we can notice that the results of the method that uses vgg19 as encoder are unconvincing. This indicates that the features extracted in this part are not pertinent. On the other hand, ResNet50 and MobilNetV2 encoders make the results more convincing and closer to the ground truth. This allows us to deduce the importance of the encoder part in the first place and the decoder part in second place. Future works will focus on the same area, and we will try to develop a new U-Net like architectures with enhancing the encoder part to get more results better than the previous ones.

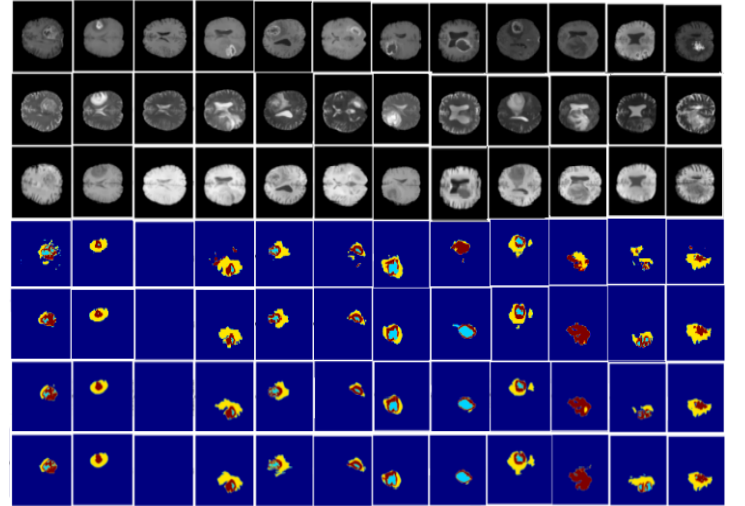


Fig. 1. Qualitative results obtained from test sub-set of BraTS2020 of each approach proposed in our paper, up to down: T1 image, T1ce image, T2 image, Vgg19+AttD, ResNet50+AttD, MobilNetV2+AttD, Ground Truth.

## V. CONCLUSION

The application of advanced technologies, particularly artificial intelligence, and machine learning improves healthcare outcomes related to brain tumor diagnosis and treatment. To this end, we present three automatic encoder-decoder methods for brain tumor segmentation. We based on the well-known pre-trained models vgg19, ResNet50, and MobileNetV2 as feature extractors using fine-tuning transfer learning techniques. Additionally, the Attention mechanism is employed in the decoder part to focus on the right pixels. The proposed models have been trained and evaluated on the available open-access dataset BraTS 2020 using some segmentation metrics such as accuracy and DSC. The outcomes obtained are significant and acceptable to improve them in future works and adopt our 2D models for 3D brain tumor segmentation.



## REFERENCES

- [1] Almahfud, Mustofa Alisahid, et al. "An effective MRI brain image segmentation using joint clustering (K-Means and Fuzzy C-Means)." 2018 International Seminar on Research of Information Technology and Intelligent Systems (ISRITI). IEEE, 2018.
- [2] Cui, B.; Xie, M.; Wang, C. A Deep Convolutional Neural Network Learning Transfer to SVM-Based Segmentation Method for Brain Tumor. In Proceedings of the 2019 IEEE 11th International Conference on Advanced Infocomm Technology (ICAIT), Jinan, China, 18–20 October 2019, pp. 1–5.
- [3] Chen, W.; Qiao, X.; Liu, B.; Qi, X.; Wang, R.; Wang, X. Automatic brain tumor segmentation based on features of separated local square. In Proceedings of the 2017 Chinese Automation Congress (CAC), 20–22 October 2017, Jinan, China.
- [4] Hatami, T.; Hamghalam, M.; Reyhani-Galangashi, O.; Mirzakuchaki, S. A Machine Learning Approach to Brain Tumors Segmentation Using Adaptive Random Forest Algorithm. In Proceedings of the 2019 5th Conference on Knowledge Based Engineering and Innovation (KBEL), 28 February–1 March 2019, Tehran, Iran.
- [5] Fulop, T.; Györfi, A.; Csaholczi, S.; Kovacs, L.; Szilagy, L. Brain Tumor Segmentation from Multi-Spectral MRI Data Using Cascaded Ensemble Learning. In Proceedings of the 2020 IEEE 15th International Conference of System of Systems Engineering (SoSE), 2–4 June 2020 Budapest, Hungary.
- [6] Shen, D.; Wu, G.; Suk, H.-I. Deep Learning in Medical Image Analysis. *Annu. Rev. Biomed. Eng.* 2017, 19, 221–248.
- [7] Qayyum, A.; Anwar, S.M.; Awais, M.; Majid, M. Medical Image Retrieval using Deep Convolutional Neural Network. arXiv 2017, arXiv:1703.08472.
- [8] Pereira, S.; Pinto, A.; Alves, V.; Silva, C.A. Brain Tumor Segmentation Using Convolutional Neural Networks in MRI Images. *IEEE Trans. Med. Imaging* 2016, 35, 1240–1251.
- [9] Zhao, X.; Wu, Y.; Song, G.; Li, Z.; Fan, Y.; Zhang, Y. Brain tumor segmentation using a fully convolutional neural network with conditional random fields. In *International Workshop on Brainlesion: Glioma, Multiple Sclerosis, Stroke and Traumatic Brain Injuries*; Springer: Cham, Switzerland, 2016; pp. 75–87.
- [10] Wang, G.; Li, W.; Ourselin, S.; Vercauteren, T. Automatic brain tumor segmentation using cascaded anisotropic convolutional neural networks. In *International MICCAI Brainlesion Workshop*; Springer: Cham, Switzerland, 2017; pp. 178–190.
- [11] Aboussaleh, Ilyasse, et al. "Brain tumor segmentation based on deep learning's feature representation." *Journal of Imaging* 7.12 (2021): 269.
- [12] Ronneberger, Olaf, Philipp Fischer, and Thomas Brox. "U-net: Convolutional networks for biomedical image segmentation." *International Conference on Medical image computing and computer-assisted intervention*. Springer, Cham, 2015.
- [13] Liu, Hongying, et al. "CU-Net: Cascaded U-Net with loss weighted sampling for brain tumor segmentation." *Multimodal Brain Image Analysis and Mathematical Foundations of Computational Anatomy*. Springer, Cham, 2019. 102–111.
- [14] Aboelenen, Nagwa M., et al. "HTTU-Net: Hybrid Two Track U-Net for automatic brain tumor segmentation." *IEEE Access* 8 (2020): 101406–101415.
- [15] Aboussaleh, Ilyasse, et al. "Inception-UDet: an improved U-Net architecture for brain tumor segmentation." *Annals of Data Science* (2023): 1–23.
- [16] Keetha, Nikhil Varma, and Chandra Sekhara Rao Annavarapu. "U-Det: A modified U-Net architecture with bidirectional feature network for lung nodule segmentation." arXiv preprint arXiv:2003.09293 (2020).
- [17] Pravitasari, Anindya Apriliyanti, et al. "UNet-VGG16 with transfer learning for MRI-based brain tumor segmentation." *TELKOMNIKA (Telecommunication Computing Electronics and Control)* 18.3 (2020): 1310–1318.
- [18] Zhang, Jianxin, et al. "Attention gate resU-Net for automatic MRI brain tumor segmentation." *IEEE Access* 8 (2020): 58533–58545.
- [19] Aboussaleh, Ilyasse, et al. "Efficient U-Net Architecture with Multiple Encoders and Attention Mechanism Decoders for Brain Tumor Segmentation." *Diagnostics* 13.5 (2023): 872.
- [20] Aboussaleh, Ilyasse, et al. "3D U-NetR+: A 3D hybrid Semantic Architecture using Transformers for Brain Tumor Segmentation with MultiModal MR Images." *Results in Engineering* (2024): 101892.
- [21] Wu, Xinheng, et al. "Unsupervised brain tumor segmentation using a symmetric-driven adversarial network." *Neurocomputing* 455 (2021): 242–254.
- [22] Menze, Bjoern H., et al. "The multimodal brain tumor image segmentation benchmark (BRATS)." *IEEE transactions on medical imaging* 34.10 (2014): 1993–2024.
- [23] Bakas, Spyridon, et al. "Advancing the cancer genome atlas glioma MRI collections with expert segmentation labels and radiomic features." *Scientific data* 4.1 (2017): 1–13.
- [24] Bakas, Spyridon, et al. "Identifying the best machine learning algorithms for brain tumor segmentation, progression assessment, and overall survival prediction in the BRATS challenge." arXiv preprint arXiv:1811.02629 (2018).
- [25] Kronberg, Raphael M., et al. "Optimal acquisition sequence for AI-assisted brain tumor segmentation under the constraint of largest information gain per additional MRI sequence." *Neuroscience Informatics* (2022): 100053.
- [26] Sudre, Carole H., et al. "Generalised dice overlap as a deep learning loss function for highly unbalanced segmentations." *Deep learning in medical image analysis and multimodal learning for clinical decision support*. Springer, Cham, 2017. 240–248.
- [27] Fang, Longwei, and Huiguang He. "Three pathways U-Net for brain tumor segmentation." *Pre-conference proceedings of the 7th medical image computing and computer-assisted interventions (MICCAI) BraTS Challenge*. Vol. 2018. 2018.
- [28] W. Chen, B. Liu, S. Peng, J. Sun, and X. Qiao, "S3D-UNET: Separable 3D U-Net for brain tumor segmentation," in *Proc. 4th Int. Workshop, BrainLes, Held Conjunct. (MICCAI)*, in *Lecture Notes in Computer Science*, vol. 11384. Granada, Spain: Springer, 2019.
- [29] Chen, Shengcong, Changxing Ding, and Minfeng Liu. "Dual-force convolutional neural networks for accurate brain tumor segmentation." *Pattern Recognition* 88 (2019): 90–100.